Review

Insights into Induction Heating Processes for Polymeric Materials: An Overview of the Mechanisms and Current Applications

Alberto Mariani [1,2] and **Giulio Malucelli** [2,3,*]

1   Department of Chemical, Physical, Mathematical and Natural Sciences, University of Sassari, Via Vienna 2,
     07100 Sassari, Italy; mariani@uniss.it
2   Consorzio Interuniversitario per la Scienza e Tecnologia dei Materiali, INSTM, Via Giusti 9,
     50121 Firenze, Italy
3   Department of Applied Science and Technology, Politecnico di Torino, Viale Teresa Michel 5,
     15121 Alessandria, Italy
*   Correspondence: giulio.malucelli@polito.it; Tel.: +39-0131229369

Abstract: In polymer systems, induction heating (IH) is the physical outcome that results from the exposure of selected polymer composites embedding electrically-conductive and/or ferromagnetic fillers to an alternating electromagnetic field (frequency range: from kHz to MHz). The interaction of the applied electromagnetic field with the material accounts for the creation of magnetic polarization effects (i.e., magnetic hysteresis losses) and/or eddy currents (i.e., Joule losses, upon the formation of closed electrical loops), which, in turn, cause the heating up of the material itself. The heat involved can be exploited for different uses, ranging from the curing of thermosetting systems, the welding of thermoplastics, and the processing of temperature-sensitive materials (through selective IH) up to the activation of special effects in polymer systems (such as self-healing and shape-memory effects). This review aims at summarizing the current state-of-the-art of IH processes for polymers, providing readers with the current limitations and challenges, and further discussing some possible developments for the following years.

Keywords: induction heating; reaction mechanisms; eddy currents; magnetic polarization; applications

1. Introduction

The manufacturing of any material, and in particular polymers and their composites, requires some processing steps that usually involve heating: for instance, granules of thermoplastics are fed to extrusion or injection molding machines and heated according to a specific temperature program, aiming to achieve the rheological characteristics necessary for their processing. Further, thermosetting resin systems are generally heated to selected temperatures to be cured [1]. Heating is often provided by a standard heating source (such as flame, electrical resistance, oven, autoclave, etc.), which is effective for transferring the heat to the material to be processed, hence allowing for the manufacturing of the material itself. Although conventional heating is a very well-assessed procedure, already adopted in the polymer processing industries, it shows some limitations/drawbacks, which generally include long processing protocols, possible degradation phenomena when the heat transfer is not well controlled, and rather high energy consumption, among others.

A possible alternative approach is induction heating (IH), a contactless, very effective method that is becoming increasingly employed for several manufacturing processes [2], thanks to its advantages, namely: good reproducibility, fast heating rate, high precision in localizing the heating, and instant start/stop (without the need for a warm-up for each performed heating cycle). Generally speaking, any basic induction system consists of one or more inductors (supplied with alternating current and working at different frequencies)

and material workpieces to be heated (Figure 1). The resulting fast-oscillating magnetic field generates the eddy currents in the workpiece due to the Joule effect, hence determining ohmic heat losses inside the workpiece. Further, the presence of ferromagnetic materials (i.e., the so-called susceptors) can be exploited for generating heat through magnetic hysteresis effects.
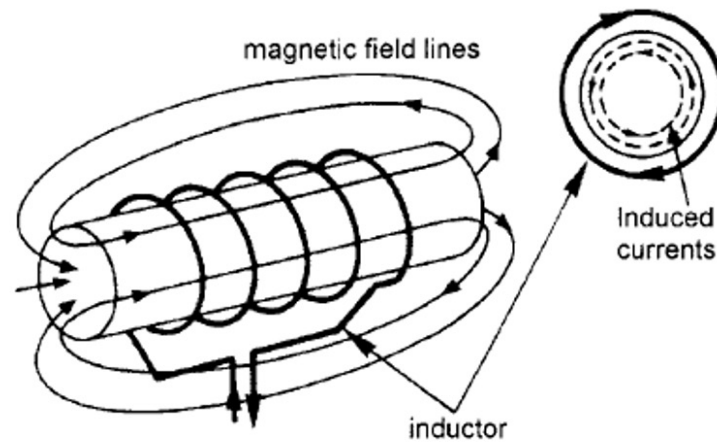
Figure 1. Induction heating setup. Reprinted with permission from [3].

The present work aims at summarizing the current state-of-the-art related to induction heating and its use in polymer-based systems, providing the reader with the existing applications and discussing some limitations and possible advances for the future. This technique has been investigated for polymer-based systems only recently, and therefore it is quite new for this class of materials. Its interest gathered in academia is well-documented by the growing number of articles published in peer-review journals and indexed conference proceedings during the last ten years (Figure 2).
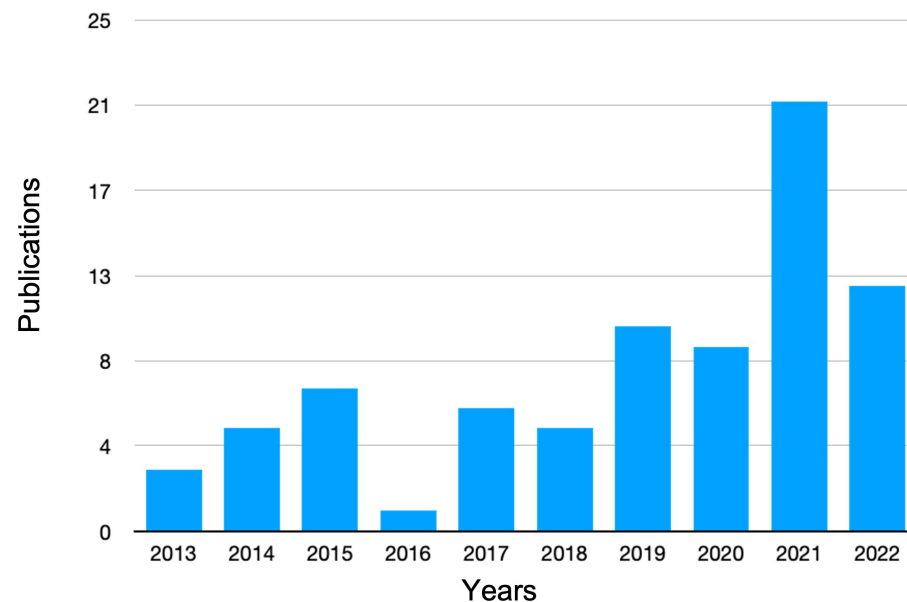
Figure 2. Number of publications (from 2013 to 2022) in peer-reviewed journals and indexed conference proceedings dealing with induction heating for polymer systems (data collected from the Web of Science™ database, accessed on 25 May 2023).

For the reader's convenience, Figure 3 displays a flowchart describing the outline and organization of the review paper.
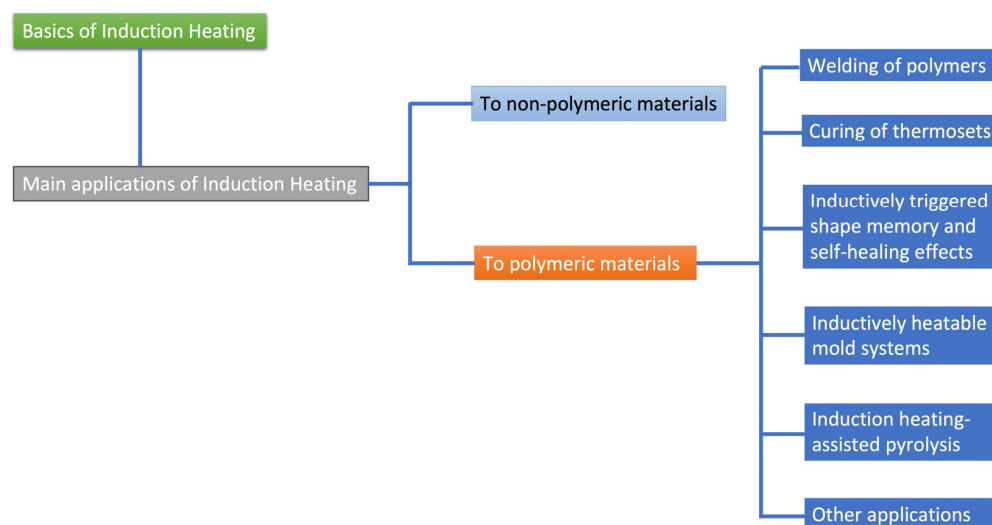
**Figure 3.** Flowchart describing the outline and organization of the review.

2. Basics of Induction Heating

When a magnetically susceptible medium (i.e., a susceptor) is immersed in an alternating magnetic field, radiofrequency energy is delivered directly to the material and locally converted into heat with only small energy losses due to convection, conduction, or thermal radiation. The three main electromagnetic dissipation phenomena responsible for the conversion of radiofrequency (rf) energy into heat, which depend on the nature of the susceptor, are (i) hysteresis heating, in the case of ferromagnetic (FM) materials, which is due to hysteresis phenomena generated during alternating magnetic field cycles (Figure 4); (ii) the relaxation mechanism of Néel, due to relaxation losses occurring in superparamagnetic (SPM) nanoparticles; and (iii) Joule heating due to eddy currents (or Foucault currents) occurring in electrically conductive materials.
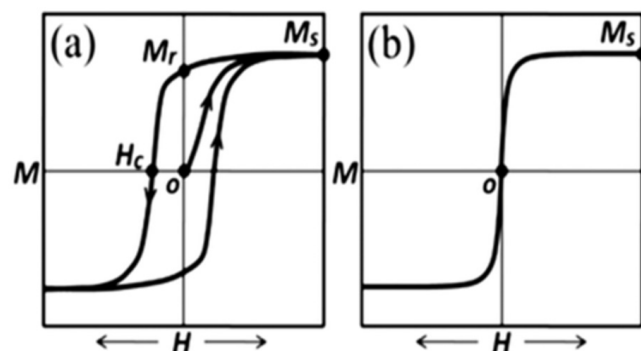
Figure 4. Schematic illustration of (**a**) a typical hysteresis loop of an array of FM nanoparticles and (**b**) a typical curve for a superparamagnetic sample. (M_r: residual magnetization; M_s: magnetization retained by the material in its magnetically saturated state; H_c: coercive field). Reproduced with permission from [4].

The greater the hysteresis area, the higher the energy absorbed per unit mass and, thus, the heat produced. The contribution of hysteresis to heat production is not present in the case of superparamagnetic particles (SPMs; Figure 4b), which dissipate electromagnetic energy through the mechanism known as Néel relaxation, which consists of the rotation of the individual magnetic moments of metallic nanoparticles against an applied external magnetic field, resulting in the release of heat into the system. It differs from the Brownian or Debye relaxation, which implies the rotation of the entire particle [5].

In addition to hysteresis losses and Néel relaxation phenomena, eddy currents induced by a magnetic ac field, flowing through the resistance of an electrically conductive

susceptor, dissipate energy by the Joule effect [6]. Unlike previous mechanisms, such currents generated by an ac magnetic field do not contribute to homogeneous heating of the conductor but concentrate heat mainly on the surface of the susceptor (according to a skin-depth effect) [7].

The heat station employs a capacitor and a coil to heat the sample. Energy is transferred to the workpiece through the induction coil. The efficiency depends on the distance between the coil and the sample, the coil geometry, and the type of sample. Maximum efficiency is observed when the coil and sample are as close as possible (Figure 5).
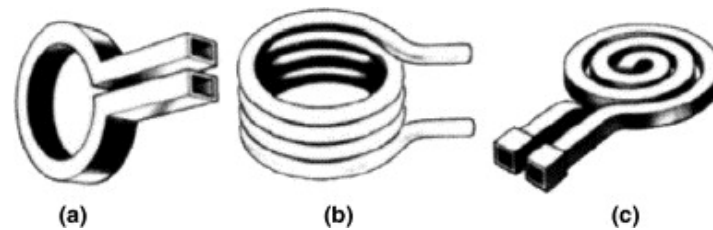
Figure 5. Basic coil shapes. (**a**) Single turn, (**b**) solenoid, and (**c**) pancake. Reproduced with permission from [8].

Voltage, power, and frequency are the main parameters influencing induction heating efficiency. In particular, its maximum is achievable by operating at the resonant frequency of the induction coil; thus, its characteristics should match those of the power source [8]. The frequency strongly depends on the type of application and the material to be treated and can vary from a few Hz for high-power systems (for example, several MW for metal melting) to hundreds of kHz and a few MW (for surface heat treatments).

An important feature of induction heating is that heat is produced within the sample as a response to applying the magnetic field. However, the properties of the material to be heated play a crucial role in defining how and where heat is produced. Indeed, the material itself can act as the susceptor [9], this occurrence being generally desirable because of the absence of additional material that may contaminate the sample and needs to be removed after the synthesis.

To induce eddy currents in the sample, the presence of a loop is necessary. Thus, heat is generated according to Joule's law, $E = (I)^2 Rt$, where I is the current, R is the resistance, and t is the time of exposure to the magnetic field.

Three main mechanisms responsible for heating have been identified, which also differ in the location where they occur—the joule loss, junction heating, and hysteresis loss—the relative importance of which depends on the type of material subjected to irradiation.

The Joule loss is related to the Joule effect and depends on the electrical resistance of the material. It assumes particular importance in the presence of partially conducting materials (e.g., fibers), which are heated by irradiation.

As for junction heating, this can be of various kinds. In particular, it may depend on whether the non-conductive material contains particles that are instead, which in turn may be close to each other or not. In the case where the particles are in contact, heating occurs due to the resistance at the junction and the voltage drop across it. When, on the other hand, the conductive particles are further apart (but not too distant, however) and an alternating magnetic field is applied, a potential difference is generated between them, and a capacitor effect is created. In this case, dielectric heating occurs due to the movement of charges and rotation of the molecules between the conductive particles.

As for hysteresis loss, this takes place only in the presence of magnetic materials. Specifically, the latter tend to orient themselves so that their dipoles are aligned with those of the applied magnetic field. When this is alternating, magnetic particles tend to follow its changes in direction by generating heat due to the resulting friction (Figure 6).
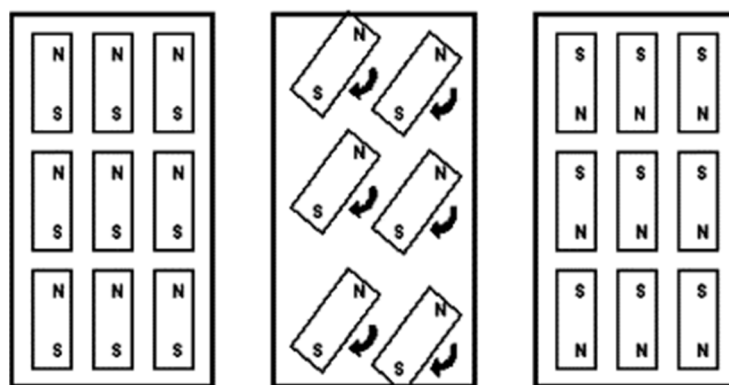
Figure 6. Hysteresis loss mechanism: dipoles of magnetic particles rotate following the alternating magnetic field; heat is generated due to friction. Reproduced with permission from [8].

The skin effect is another heating mechanism that occurs when an alternating current tends to avoid passing through the center of a solid conductor and is limited to conduction near the surface. It is caused by opposing eddy currents induced by the changing magnetic field resulting from the alternating current.

3. Applications of Induction Heating to Non-Polymeric Materials

Although it is not the focus of the present review, the authors believe that a brief description concerning the applications of IH to non-polymeric materials would help the reader to better understand the phenomena behind the technique and may provide useful suggestions to be applied to polymer systems.

Largely because of their ease of recovery and reuse, magnetic nanoparticles (MNPs) have been used in both homogeneous and heterogeneous catalysis for several years. However, although their ability to dissipate heat during exposure to a remote rf has long been known, this characteristic has only been exploited recently. In particular, their ability to heat up quickly due to their radiofrequency exposure is ideal in flow chemistry, where the residence time of the reactant on the catalyst is generally short.

In addition, the homogeneous heating of such a catalyst operating in contact with a continuous stream of reactants is handled much more quickly and efficiently by IH than by conventional heating systems.

From this point of view, the studies carried out since 2010 by Ceylan et al., who reported using Fe_2O_3/Fe_3O_4@SiO_2; MagSilica, impregnated with nanoparticles of Pd[16] or Au[40], should be noted. Specifically, the research focused on the ability of radiofrequency-powered superparamagnetic MagSilica nanoparticles to act as heating agents for a wide range of stoichiometric reactions in flow chemistry [10–12].

The studies of Kirschning's group have paved the way for several recent results in the field of inductively heated catalyst transformations under flow conditions [13,14].

The use of iron microparticles allows local control and heating of the catalyst due to both eddy currents and hysteresis losses, with positive effects on process efficiency. Finally, the rapid rate of catalyst heating/cooling ensured by induction heating has been exploited to demonstrate the easy formation of on-demand products [15].

By their nature, endothermic processes benefit most from the high efficiency of induction heating. The fast transition from heating to cooling and the ability to localize rf energy typical of this technology limits not only the cost and environmental impact of the processes but also the formation of unwanted byproducts. In particular, the efficiency of heat transfer due to convection, conduction, and radiation are physical limitations to process rate, especially in reactors with insufficiently large surface area. This results in long start-up times, especially in systems with high heat capacity and low adiabatic efficiency.

Aasberg-Petersen et al. reported that only about half of the heating supplied in conventional form is utilized by the system. From this point of view, rf heating technology

is certainly more efficient in terms of energy, product quality, process safety, and precise control of the power used [15].

Unlike in endothermic processes, in exothermic ones, the use of induction heating has been less studied because the control of the process appears to be more complicated. In fact, once a pulse of energy is received to initiate the reaction, it tends to occur spontaneously due to the heat released by the reaction itself. However, the ability to precisely control the duration of the radio frequency pulse, and thus the amount of external energy to be supplied to the system from time to time, promises exciting applications that should deserve more interest from researchers. In particular, the modulation of pulse intensity and duration, and the possibility of using even nanoscale susceptors, hint at applications in which local temperature control is much better than in traditional heating.

In fact, if local heating can be finely controlled and adjusted almost in real-time, any sudden rise in temperature due to the exothermicity of the reaction can be limited and properly redirected. In particular, in the case of hot spot formation, it can be harnessed as an additional energy source, with advantages in terms of time, cost, and environmental impact.

In 2015, Meffre et al. reported using induction heating in heterogeneous catalysis for obtaining hydrocarbons by hydrogenation of carbon monoxide. For this purpose, nanoparticles (Fe@FeCo and Fe@Ru; average diameter about 12.3 ± 1 nm) consisting of a ferromagnetic (iron) core and a catalytically active shell comprising FeCo or Ru were prepared [16].

In 2016, Bordet et al. reported applying the induction heating technique to "cold catalysis" to produce synthetic natural gas using iron carbide nanoparticles subjected to an alternating magnetic field. The use of induction heating in the presence of a high thermal conductivity susceptor allowed for very rapid heating and cooling rates resulting in improved catalyst stability and process parameter control [17].

The main domestic applications of induction heating concern kitchen hobs, which are not only characterized by improved heating times and efficiency but also lower surface temperatures, with advantages in terms of safety, as food is not burned. The appliances used in Europe and America are characterized by power up to 4 kW, while those on the Asian market generally have 2 kW of output power.

Other small-scale applications concern handicrafts and, more particularly, the processing of metals, especially aluminum and copper, which can be easily melted using equipment operating at frequencies between 20 and 100 kHz [18].

The last major area of application for induction heating is in the medical field. Specifically, it was initially used as a fast method for sterilizing equipment but is gradually finding new uses for other applications, including low-invasive therapies. For example, its use in treating some forms of cancer by hyperthermia has been reported. Specifically, this is a thermal treatment, operated at temperatures above 50 °C, that removes cancerous tissue while minimizing damage to surrounding healthy tissue. Compared with the traditional technique, advantages are reported due to lack of direct contact, reduced invasiveness, and better power control. To this end, ferromagnetic materials (including fluids containing nanoparticles) are used and placed near the tissue to be treated [19].

4. Applications of Induction Heating for Polymeric Materials

So far, induction heating of polymer systems has been successfully exploited for different uses that will be thoroughly described in the following paragraphs.

4.1. Induction Welding of Thermoplastic Systems

The welding of polymers and polymer composites has attracted significant interest from the academic community, as witnessed by the many scientific papers published so far [20–23]. In a general overview, the welding is carried out by heating the parts to be joined beyond their melting temperatures, putting them in contact (through the application of pressure), and finally cooling down the being-formed joint, keeping pressure until the material solidifies again, hence consolidating [24–27].

The HI-assisted welding exploits the presence of a susceptor directly located in the bonding area: depending on the type of welding, different materials can be utilized as susceptors, such as ferromagnetic particles, carbon fibers, and metal meshes; when hybrid polymer–metal systems are welded, it is possible to employ the metal part of the joint acting as susceptor [28–30]. Several parameters affect the overall induction heating welding process, namely: welding time, welding pressure, frequency of the applied magnetic field, generator power, and cooling time [31–33].

The IH-assisted welding can be continuous (dynamic—Figure 7) or discontinuous (static), according to the possibility of moving either the coil or the workpiece during the welding and consolidation steps [8]. Comparing the two processes highlights the higher ease of performing discontinuous welding, although the continuous technique exhibits lower cycle times and the possibility of welding complex geometries. Additionally, there exists an intermediate method, indicated as semi-continuous IH welding, which exploits a static system that concurrently performs both heating and consolidation steps; then, the being-formed joint is moved to the welding location [29]. IH welding usually works with frequencies of the applied magnetic field between 200 and 1000 kHz, although higher frequencies (not exceeding 14 MHz) can be exploited when the hysteresis cycle of the employed magnetic particles is quite small and, therefore, the transformation of magnetic energy into heat is not very effective [3,22].
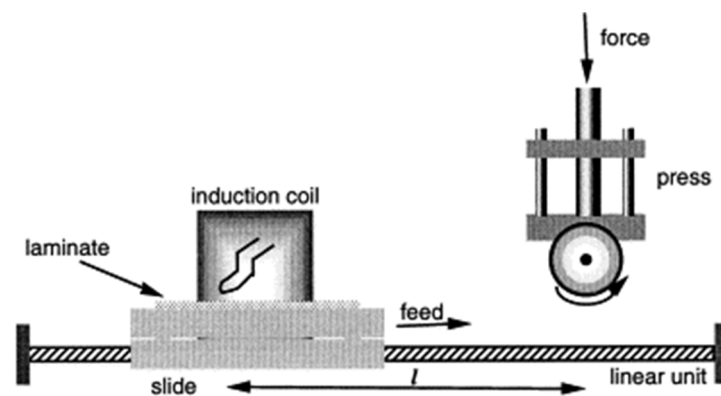
Figure 7. Scheme of the continuous induction heating-assisted welding process. Reprinted with permission from [31].

The three key heat fluxes that affect the continuous induction heating-assisted welding process are schematized in Figure 8.
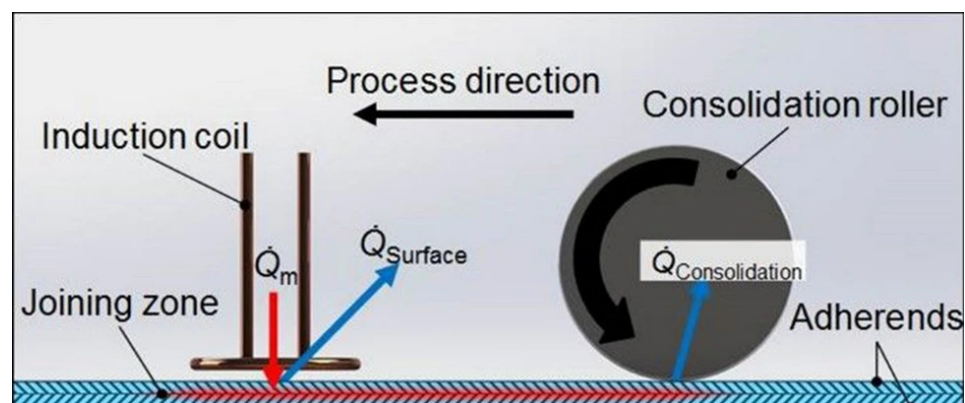
Figure 8. The three key heat fluxes that affect the continuous induction heating-assisted welding process. $\dot{Q}_m$ is the heat input resulting from the induction coil, $\dot{Q}_{surface}$ is the heat removed from surface cooling, and $\dot{Q}_{consolidation}$ is the heat removed by conduction through the consolidation roller. Reprinted from [34] under Creative Commons CC BY License.

As shown in Figure 9, when the polymer is exposed to the heating under the coil (step 1), the temperature increases up to a maximum value (Θ_1) that corresponds to the conclusion of the heating step (at time t_1). Θ_1 should fulfill two opposite requirements: it should be below the temperature, at which the polymer starts degrading, and beyond the welding temperature, as the workpiece to be joined, upon induction heating, continuously lowers its temperature before the application of the welding pressure by the roller (where Θ_2 is achieved at t_2). This is due to the heat transferred to the surroundings by convection and conduction phenomena.
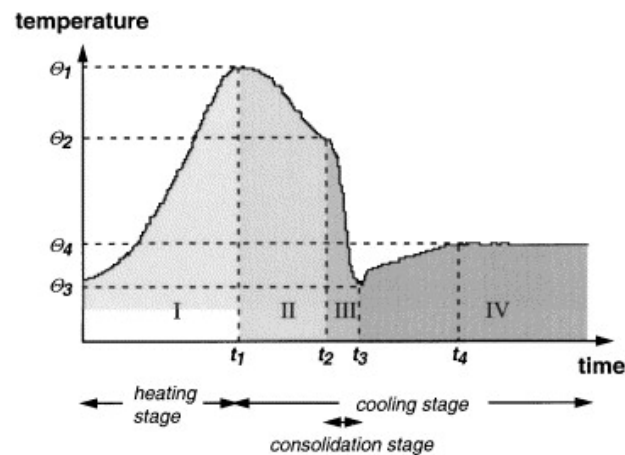
Figure 9. Usual temperature vs. time profile of the continuous induction heating-assisted welding process. Reprinted with permission from [31].

After the application of the welding pressure by the roller (that is usually water-cooled), Θ_3 should be low enough to favor the consolidation of the joint, preventing its delamination. Then, a slight temperature increase to Θ_4 takes place after the application of the welding pressure because of the residual heat that is accumulated in the joint. In order to limit the appearance of defects in the joint, Θ_4 should be as much as possible below the recrystallization temperature of the polymer parts, which would cause shrinkage phenomena and subsequently warpage and/or cracking; therefore, usually, compressed air (provided by an air jet nozzle) is applied for further cooling the joint, keeping its temperature below Θ_4. This strategy allows for creating a heating gradient through the thickness of the joint, hence locating the highest temperature at the bond line rather than on the top surface of the joint [32]. This way, it becomes possible to employ higher generator powers without inducing the occurrence of degradation phenomena on the polymer top surface, thus also not compromising its aesthetics.

Unlike continuous induction heating-assisted welding, which is more suitable for applications at a large scale, the discontinuous process fits better applications at a small scale. In this context, the first pioneering work dates to 1989 [35] and investigates the static induction heating-assisted welding of polyetheretherketone (PEEK) using susceptors made of carbon fibers. Working at low temperatures accounted for an unsatisfactory bonding strength, which increased at higher temperatures, despite the occurrence of some degradation phenomena in the welding area. Additionally, adding further metallic susceptors in the bond line decreased the joint strength.

Stokes, in 2003, proposed to perform IH-assisted discontinuous welding by using commercially available particulate susceptors (Emaweld®, from Emabond Systems, Auburn Hills, MI, USA) containing proprietary ferromagnetic particles [36]. The welding was performed using frequencies in the range of 3–14 MHz on different polymer parts, namely polycarbonate, poly(butylene terephthalate), and polypropylene. Their weld strengths were as high as 30.1, 26.0, and 17.6 MPa, respectively. However, the relatively high ferromagnetic particle concentrations in the bond areas lowered the maximum bond strength. In a further research effort, Kagan and Nichols [37] applied the same susceptors for welding nylon 6

composites containing 33 wt.% of glass fibers ("cereal bowl"-shaped); HI-assisted welding was found to improve the burst strength of the joints by 25%.

Suwanwatana and co-workers investigated the IH-assisted welding of polysulfone embedding Ni particles of different sizes as susceptor material (namely, 22 μm, 3 μm, 0.7 μm, and 79 nm) at relatively high loadings (i.e., 10–20 vol.%, which correspond to 44 and 64 wt.%, respectively) [38].

The obtained bond strengths were comparable to those attained with a standard autoclave process but with one order of magnitude decrease in cycle times. EDS analyses allowed for assessing the extent of adhesive failure (i.e., through Ni particle debonding) and cohesive failure (i.e., through matrix cracking) associated with the polysulfone fracture during shear strength tests: the adhesive failure was found to increase with increasing particle loading and reducing particle size.

Then, Knauf and co-workers [39] were the first to propose low-frequency induction heating (carried out at 200 Hz) for sealing poly(methylmetacrylate) microfluidic systems using a very thin (i.e., 5 μm) Ni-plated coating as a susceptor. The best results in terms of mechanical resistance of the microfluidic devices were reached by using pulse induction heating and applying 45 kPa bonding pressure.

To limit the issues related to the different thermal expansion coefficients in hybrid joints (i.e., made of metal (steel DC01 or aluminum $AlMg_3$) and carbon fiber-reinforced composites—selected polymer matrices: polyamide 66 and PEEK), Mitschang and co-workers [29] proposed a specific coil consolidation setup, which allowed for achieving shear, tensile strengths of 14.5 and 20 MPa, respectively, for the joints between carbon fiber-reinforced polyamide 66 and aluminum, and carbon fiber-reinforced PEEK and steel.

Very recently, Martin and co-workers [40] investigated the effectiveness of different susceptors made of Fe, Ni, and Fe_3O_4 particles in polypropylene (PP) and PEEK matrices. On the basis of the magnetic field amplitude produced by the welding setup, the thermal properties of the polymers and particles used for the susceptor and the magnetic hysteresis of the magnetic particles allowed for predicting the optimum heating rates. Additionally, the tests performed on the selected polymer matrices and susceptors were exploited for experimentally verifying the developed models. In particular, Ni was the most suitable susceptor material for PP, while magnetite was the most preferable for PEEK.

In a further research effort, Wang and co-workers [41] designed and prepared carbon fiber susceptors (0.2 mm nominal thickness) made of 5-hardness plain woven carbon fiber fabric and polyetheretherketone resin films, which were employed in carbon fiber-reinforced polyetheretherketone laminates. This way, it was possible to exploit carbon fibers both as reinforcement and as suitable susceptors. Aiming at predicting the temperature distribution in the joints and describing the heating features of the susceptors, a transient three-dimensional finite element model was developed. The obtained results demonstrated that, at the welding interface, the temperature distribution was not homogeneous because of edge effects. In particular, unlike the high-temperature edge area that exhibited variations of the slope of the temperature profiles with welding time, the central low-temperature area of the welding interface was almost uniformly heated, with an increased heating rate with increasing the input current. Further, the IH process accounted for the appearance of different welding defects in the joints, both at the macro (with the formation of unfused gaps) and micro (with extended porosity) scale.

4.2. Curing of Thermosetting Systems

The possibility of curing thermosets has always represented a key factor, especially at the beginning in military and aeronautic applications, for which in situ repairing of thermosetting-based composites is a very demanding issue. In this context, the use of induction heating has proved to be very reliable and exploitable. The first pioneering paper from Fink and co-workers, 1999 [42], who investigated the IH curing process (using copper or steel mesh susceptors) for repairing a composite integral armor using a typical room-temperature-curing epoxy system (namely, Hysol EA9394 from Henkel). Both sides

of copper/steel mesh rectangular strips were wetted with the adhesive and then positioned in the bond area. Additionally, a wooden applicator was employed for applying the adhesive onto the adherends' corresponding mating surfaces. As assessed by differential scanning calorimetry (DSC) analyses, the epoxy adhesive achieved a degree of cure of 0.8 in less than 12 min at 80 °C, hence indicating a significantly lower curing time provided by the induction heating process concerning the standard curing at room temperature (which achieved almost the same degree of cure after about 120 h). Finally, the use of these susceptors did not negatively impact the mechanical performances of the bond line, as demonstrated by shear strength tests.

Miller and co-workers [43] demonstrated the suitability of FeCo/(Co,Fe)$_3$O$_4$ crio-milled nanoparticles, induction-heated at 267 kHz and 2 kW power (20.0 kA/m field amplitude), for curing a diglycidylether of bisphenol F resin. In particular, a nanoparticle loading (average particle diameter: 9 nm) of 1.36 vol.% accounted for heating rates as high as 1 K/s, reaching temperatures beyond 100 °C in about 70 s, effectively curing the epoxy system.

Ye et al. [44] investigated the IH curing behavior of opaque composites comprising thiol-acrylate or thiol-ene resins and incorporating 1 wt.% of AIBN and 1 wt.% of magnetic particles (i.e., Ni nanoparticles or Co microparticles) as susceptors, and further added multiwalled carbon nanotubes (loadings between 0.5 and 1.5 wt.%). The thiol–ene systems reached full conversion within 1.5 min and 1 h, based on the field intensity and the composition: the maximum reaction temperature decreased from 146 to 87 °C, referring to 8 and 3 kW power of the induction heater, respectively. Further, compared to thiol-ene systems, the thiol–acrylate counterparts were faster in reaching full conversion (between 0.6 and 30 min), exhibiting maximum temperatures from 139 to 86 °C according to the selected power of the induction heater.

Quite recently, Vashisth and co-workers [45] demonstrated that it is possible to exploit IH for making the continuous processing of epoxy pre-pregs (from diglycidyl ether of bisphenol F), incorporating either 5 wt.% carbon nanotubes or 60 vol.% carbon fibers. In particular, the thermal response of the prepared pre-pregs was found to be strictly related to the adopted experimental parameters (i.e., the geometry of the IH apparatus and frequency, the thermal and electrical conductivity of the pre-pregs, among others); heating rates up to 6 and 70 K/s were achieved at input powers as low as 5 W, and as high as 25 W, respectively.

Voß and co-workers [46–48] thoroughly investigated the kinetics and the mechanical behavior (in particular, the load capacity) of fiber-reinforced adhesively-bonded composite tubular joints in the presence of Mn-Zn-ferrite particles (the so-called Curie particles, used as susceptors), which were incorporated at 33.3 wt.% loading into two adhesives (namely, a two-component epoxy and a polyurethane system). The presence of the susceptors accounted for an increase in the curing kinetics of the adhesives. Additionally, better control of the temperature during the curing process was achieved; in fact, the Curie particles prevented the bond from overheating as their induced heat was limited by their Curie temperature (at which it automatically stopped). Further, as assessed by tensile tests, the joint strength was not limited by the type of the selected adhesives but rather by the structure and properties of the tubular adherends. Finally, it was possible to provide a reliable multi-physics finite element model for predicting the mechanical behavior of the tubular joints.

Very recently, the same research group assessed the feasibility of IH for: (i) the low-temperature curing of three different two-component structural adhesives (one polyurethane and two epoxy adhesives), into which Curie particles were incorporated at 33.3 wt.% constant loading [49], and for (ii) the fast curing of two two-component epoxy adhesives, using the same Curie particle loading [50,51]. Concerning the former, the heating behavior of glued-in-rod joints conditioned at −10 °C and −30 °C was compared to that of the same joints that were IH-cured starting from ambient temperature (i.e., 23 °C). Regardless of the adopted conditioning temperature, it was possible to inductively cure the structural

adhesives, achieving, in the case of the two epoxy systems containing the Curie particles, the same fracture behavior as the unfilled adhesive counterparts.

As far as the fast curing of epoxy adhesives is considered, it was possible to elaborate an appropriate kinetic model based on the data obtained from differential scanning calorimetry (DSC) analyses, which was able to predict the curing temperatures resulting from IH-accelerated curing.

4.3. Inductively Triggered Shape Memory and Self-Healing Effects in Polymer Systems

Induction heating can be successfully exploited for triggering such effects in polymer systems as self-healing abilities and shape memory transitions. As is very well known, shape memory polymer systems are smart materials capable of recovering to a defined shape (i.e., the so-called permanent shape) from a temporary shape, achieved by "freezing" a mechanical deformation. Usually, for this transition, shape memory polymer systems take advantage of such triggering mechanisms as light and heat [52].

Self-healing (or self-mending or self-repairing) polymer systems exploit different triggering mechanisms (such as covalent-bond reformation and reshuffling, diffusion, and flow, and dynamics of supramolecular chemistry, among others) for recovering from physical damages [53]. Often, healing is triggered by heating the damaged material to a specific temperature, at which some of the components of the healing system change their physical state from solid to liquid gel that, in turn, can fill the cracks, hence repairing the material.

The necessary heat either to shape memory polymers to recover from a temporary shape or for self-healing polymers to restore their usability can be provided by induction heating when suitable ferromagnetic particles are incorporated into these polymers.

As far as shape memory polymers are considered, Mohr et al. [54] were among the first to propose the use of core–shell magnetite/silica nanoparticles (at 5–10 wt.% loading) as a susceptor for two different polymer matrices, namely a polyetherurethane and a biodegradable multiblock copolymer with poly(ε-caprolactone) as the soft segment and poly(p-dioxanone) as the hard segment. Induction heating carried out on the materials' temporary shape in an alternating magnetic field (frequency = 258 kHz; field intensity = 30 kA/m) accounted for the shape memory effect, showing shape recovery rates comparable with those achieved by raising the environmental temperature.

Yakacki and co-workers [55] demonstrated the suitability of IH for triggering the shape recovery in methacrylate-based thermoset networks containing Fe_3O_4 nanoparticles at two different loadings (namely, 1 and 2.5 wt.%). The investigated composites exhibited good shape memory properties, although these latter decreased with decreasing the crosslinking density of the network and with increasing the filler loading because of the occurrence of extended irrecoverable (plastic) strains.

Very recently, Liu et al. [56] prepared poly(lactic acid)/thermoplastic polyurethane blend (weight ratio: 85/15) filaments embedding magnetite particles at different loadings (namely, 15, 20, 25, and 30 wt.%), suitable for fused filament fabrication of shape memory polymers. All composites showed excellent shape fix ratio (approaching 100%), recovery ratio (>91%), and rapid magnetic response within as short as 40 s (in the case of the highest particle loading, Figure 10), suggesting the high effectiveness of heat generation provided by the embedded magnetic particles through induction heating.

Regarding self-healing polymers triggered by IH, Adzima and co-workers [57] demonstrated the effectiveness of IH for the design of self-healable reversible polymeric networks (derived from the reaction of a trisfuran—pentaerythritol propoxylate tris(3-(furfurylthiol)propionate—with a bismaleimide—1,1'-(methylene-di-4,1-phenylene) bismaleimide) incorporating ferromagnetic particles (i.e., chromium(IV) oxide) and synthesized via the Diels–Alder reaction. In situ heating was found to occur when the networks were placed in an alternating magnetic field, exploiting the self-limiting heating behavior of the selected ferromagnetic particles; consequently, the networks reverted to a liquid (because of the retro-Diels–Alder reaction), which filled the cracks, hence repairing the

damage. It was demonstrated that the properties of the designed networks did not change even after ten cycles of damage and healing.
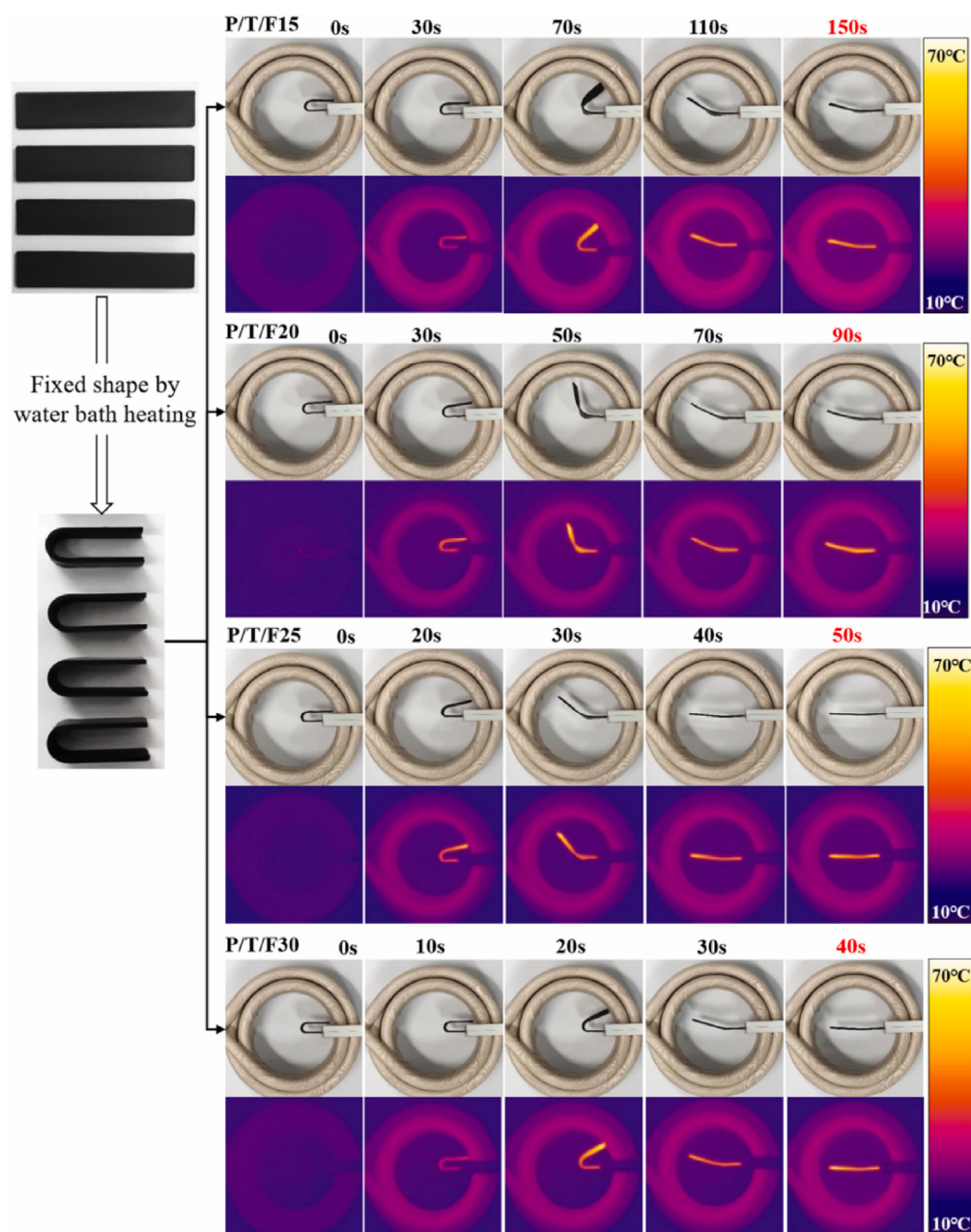

Figure 10. Shape memory behavior of the composites with different Fe_3O_4 contents triggered by magnetic field. Legend: P/T/FXX = composite made of poly(lactic acid) and thermoplastic polyurethane, containing XX wt.% of magnetite. Reprinted with permission from [56].

Quite recently [58], IH was exploited for triggering the self-healing of random, anionic polyelectrolyte copolymers consisting of di(ethylene glycol) methyl ether methacrylate and sodium-4-(methacryloyloxy)butan-1-sulfonate, synthesized by ATRP and containing oleic acid functionalized iron oxide particles as susceptor at different loadings (namely, 2, 5, 10, and 20 wt.%). As shown in Figure 11, the polyelectrolyte copolymers were able to fully self-repair after treatment in the induction oven carried out at 58 °C.
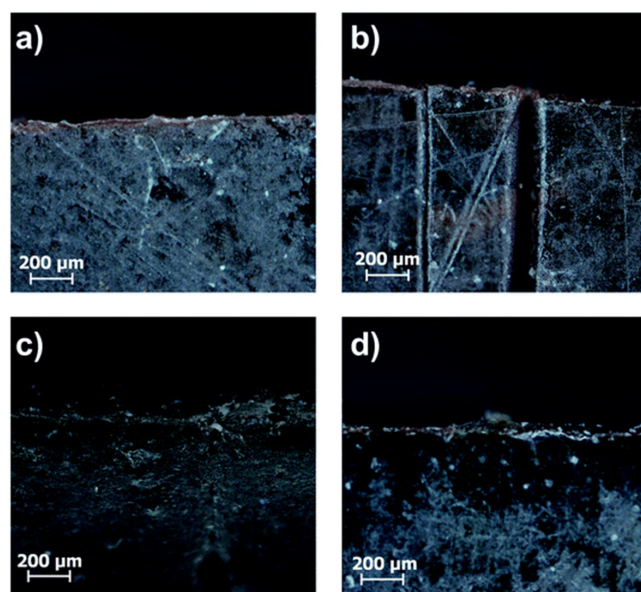
Figure 11. Microscope images of the (**a**) untreated sample containing 20 wt.% of oleic acid functionalized iron oxide particles, (**b**) the cut sample and the healed sample after (**c**) 24 h and (**d**) 48 h at 58 °C in the induction furnace. Reprinted from [58] under Creative Commons CC BY-NC 3.0 License.

Cheng et al. [59] demonstrated that it is possible to achieve fast and contactless on-demand debonding and rebonding by incorporating magnetite nanoparticles into poly(ethylene-methacrylic acid). As shown in Figure 12, upon the application of an external alternating magnetic field, the localized heat generated by the ferrimagnetic nanoparticles was able to melt poly(ethylene-methacrylic acid), hence allowing for a fast (<1 min) debonding and rebonding of the polymer adhesive. It is worth highlighting that the presence of the nanoparticles accounted for 100% recovering of the original bond strength, even after five cycles of repeated debonding and rebonding. Further, an as fast as 0.4 °C/s heating rate was observed in the presence of 20 wt.% nanoparticle loading when a 2 kW electromagnetic field generator was employed. For this adhesive formulation, just a slight decrease in the lap shear strength of the joints was observed (Figure 13), highlighting the feasibility of the proposed strategy.
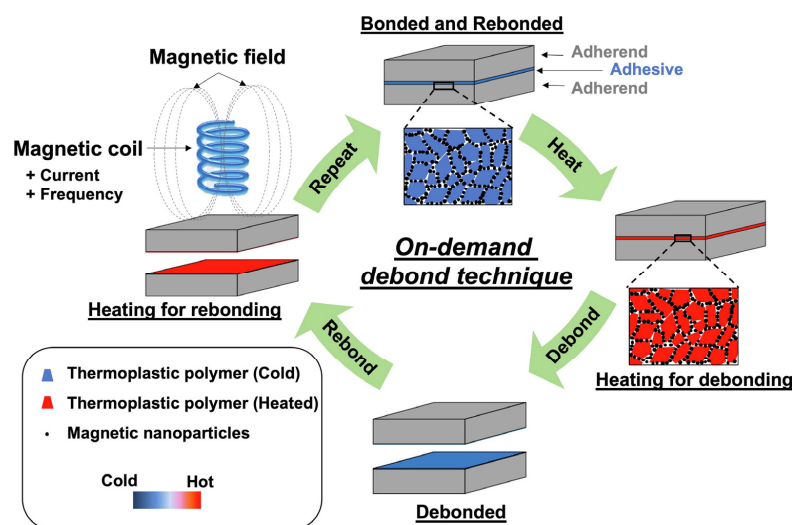
Figure 12. Scheme of on-demand detachable adhesive under alternating electromagnetic field. Reprinted from [59] under Creative Commons CC BY-NC-ND 4.0 License.
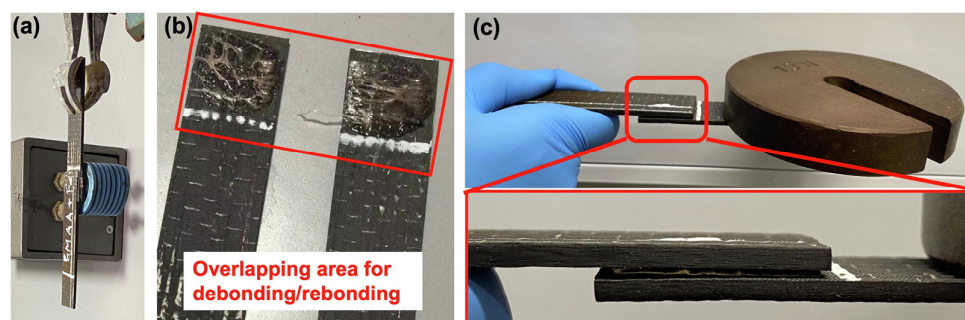
Figure 13. (**a**) Setup of debonding of adhesive-bonded joints using magnetic heating. (**b**) Image of EMAA bonded joints separated by a small finger pull force; (**c**) rebonded unidirectional carbon fiber-reinforced epoxy laminate joint carrying a deadweight. Reprinted from [59] under Creative Commons CC BY-NC-ND 4.0 License.

A similar approach was recently reported by Palanisamy and co-workers [60], who proposed a method for precisely measuring the temperature of the adhesive to avoid both underheating (which may promote inefficient bonding) and overheating (which may account for the adhesive degradation). In particular, they combined ultrasonic-guided wave sensing and optical frequency domain reflectometry for real-time monitoring of both melting and polymerization processes in a glass fiber-reinforced epoxy lap shear joint using an acrylonitrile–butadiene–styrene (ABS) copolymer (reinforced by magnetite nanoparticles at 16 wt.% loading) as the adhesive. A 6.6 kW electromagnetic field generator, operating at 200 kHz, was employed for heating the ABS copolymer, exploiting both the hysteresis losses and eddy currents originating among locally agglomerated magnetite nanoparticles. After the lap shear joint was cooled down to ambient temperature, it was found that Young's modulus of ABS regained its pristine value measured before IH, demonstrating the viability of the proposed bonding technique.

Recently, Waldmann and Keller [61] mixed high-density polyethylene with 15 vol.% carbon black and 10, 15, or 20 vol.% aluminum flakes (acting as susceptors) in a Banbury mixing unit, operating at 160 °C for 15 min. Then, they performed tensile tests on dogbone specimens, measuring the electrical resistance during mechanical testing. After the initial tensile testing, the two halves of the broken specimens were held in close geometric proximity to provide contact between the fracture surfaces, inductively heated for 20 min, cooled down to ambient temperature, and tested again. A total of 20 min of IH was enough for healing the samples containing the highest loading of aluminum flakes (i.e., 20 vol.%), both from the mechanical and electrical point of view, notwithstanding the slightly increased stiffness and lower initial electrical resistance of the healed samples when compared with the initially tested counterparts.

Kanidi and co-workers [62] demonstrated the multifunctional features (i.e., on-demand bonding and debonding, and self-healing) provided to four different thermoplastic polymer matrices (namely, thermoplastic polyurethane, polypropylene, polyamide 12, and polyetherketoneketone) embedding Fe_3O_4 nanoparticles at different loadings (2.5, 5, 7.5, and 10 wt.%). A 4–6 kW electromagnetic field generator, operating at three different frequencies (namely, 325, 446, and 575 kHz), was employed. Apart from polyetherketoneketone, which showed self-healing capabilities for longer IH times (but only when filled with the highest nanoparticle loading), all the other thermoplastic matrices could heal in less than 10 min of exposure to the electromagnetic field. Finally, both polypropylene and polyamide 12 showed on-demand bonding/debonding features, respectively, after less than 1 and 3 min exposure to the electromagnetic field.

4.4. Inductively Heatable Mold Systems for Polymers and Polymer Composites

Several efforts have been carried out to design inductively heatable mold systems for polymers and composites. This way, it is possible to develop a quick and very con-

trollable system for tool heating, as clearly demonstrated in a pioneering work dating to 2008 [63]. At present, the significant progress in inductively heatable mold systems allowed for making them available for thermosets and reactive polymers/composites and for thermoplastics [64].

Generally speaking, two mold approaches are available on the market: one mainly refers to injection molding processes, while the other is suitable for compression molding systems. The former is based on heating the tool surface using focused magnetic fields that are originated by an inductor cage surrounding the mold. It is possible to use either stainless steel (hence non-magnetic mold parts) to limit the interference with the magnetic fields or structural steel that ensures homogeneous heating in the center of the mold [65]. Conversely, for compression molding, inductors are placed in the mold; therefore, the surface of the mold is indirectly heated. This approach is very effective for manufacturing shear edges.

Chen et al. [66] assessed the feasibility and effectiveness of HI on mold surface temperature control; to this aim, a mold plate provided with four cooling channels was employed, changing the mold surface temperature from 110 to 180 °C and 110 to 200 °C; an ABS copolymer was utilized. A total of 4 and 21 s were enough to increase the temperature of the mold surface from 110 to 200 °C and to cool it to 110 °C, respectively. This way, it was possible to obtain high-gloss surfaces and weld lines with a limited extension, as observed in the injection-molded parts.

Kim and co-workers [67] implemented the induction heating method to resolve the incomplete filling issues during injection-molding nanoscale cavities. To this aim, electroforming was exploited to fabricate a prototype mold embedded with a nickel stamp equipped with nanograting structures. To enhance the filling of a cyclic olefin copolymer into the nanocavities, the authors designed an IH-assisted injection molding process; the experimental testing confirmed the possibility of obtaining nanograting structures, reducing, at the same time, the cycle times below 40 s.

Tanaka and co-workers [68] designed an induction heated mold for obtaining poly(lactic acid)/jute fiber composites. A significant decrease in cycle times was achieved, with an improvement in the mechanical properties of the resulting composites (i.e., tensile strength) concerning standard thermal cycles, due to the lower thermal stresses applied to the natural reinforcement.

4.5. Induction-Heating-Assisted Pyrolysis

Most plastics decompose when heated at 200–400 °C in an inert atmosphere. The main resulting products are in the form of gas (i.e., hydrogen, carbon oxides, ammonia, hydrocarbons), liquid (i.e., hydrocarbons, water), and solid (i.e., carbon black, ash), which are valorized in the perspective of the circular economy. As an example, regarding the use of induction heating in treating polyvinylchloride (PVC) waste, Nakanoh et al. reported various advantages of the method over traditional pyrolysis [69]. More specifically, it was found that: (i) dioxin production is particularly low because the process indirectly heats PVC inside a hermetically sealed reactor free of oxygen contamination; (ii) the high rate of heating makes it possible to limit the permanence of residues to the temperatures at which dioxins tend to form (200–300 °C); (iii) induction heating has a thermal efficiency of 85%, which is much higher than other methods using a furnace as a heat generator; (iv) there is no reduction in efficiency caused by the formation of soot; (v) various types of wastes may be treated, even when mixed with other types of materials, including inert ones; (vi) the plant can be configured to operate in continuous or in batch; and (vii) it is fully scalable and can operate in configurations ranging from personal to company use.

4.6. Other Applications

IH is currently being exploited for emerging applications that differ from those described in the previous paragraphs. In this context, recently, Qing and co-workers [70] demonstrated that the limit due to the occurrence of interfacial temperature polarization

phenomena exhibited by conventional membrane distillation processes (which may promote a lowered thermal efficiency when hot saline water is employed as the main thermal driver) could be overcome by using electrically conductive membranes. In particular, they utilized a polytetrafluoroethylene membrane spray-coated with a conductive layer of polyaniline embedding magnetite nanoparticles. A 5 W electromagnetic field generator, operating at 154 kHz, was employed. The presence of the nanoparticles in the conductive polymer coating accounted for an almost doubled heating rate (2.0 °C/s vs. 1.1 °C/s for the membrane without polyaniline but with the nanoparticles directly coated onto the polytetrafluoroethylene membrane). This finding was attributed to the creation of multiple conductive pathways or eddy current channels through the conductive polyaniline network. Further, the designed membrane exhibited an increase in the permeate flux with increasing the induction power of the generator. Additionally, the thermal and mass transport processes at the interface of the induction-heated membrane were examined by finite element analysis; the elaborated models matched well the obtained experimental results.

Hsu and co-workers [71] succeeded in overcoming the issues (namely, poor thermal conductivity, low hardness, and heating ineffectiveness) related to the use of polydimethylsiloxane for roller embossing processes, employed for replicating microstructures onto different polymeric substrates. In particular, Ni magnetic particles (having different sizes) were incorporated into polydimethylsiloxane at 70 wt.% loading; IH was provided by an external 7.5 kW generator working at 80 kHz. Compared with the mold made with the unfilled polymer, the composite counterpart could be rapidly heated from ambient temperature up to 220 °C within 1 min, with an increased heating efficiency of 134%, justifying the possibility of replacing the conventional metal molds in rolling embossing processes.

In summary, this review has underlined the potential of IH for applications ranging from polymer welding, curing of thermosets (including adhesives), triggering of shape memory and self-healing effects, polymer pyrolysis, to membrane distillation and roller embossing processes (Table 1).

Table 1. Main applications of IH in polymer science and technology.

Application	Type of Susceptor	Main Outcomes	Ref.
Induction welding of metal–polymer composite hybrid joints	Steel	- Shear tensile strengths of 14.5 and 20 MPa, respectively, for the joints between carbon fiber-reinforced polyamide 66 and aluminum and carbon fiber-reinforced PEEK and steel.	[29]
Induction welding of PEEK	Carbon fibers	- At low working temperatures, unsatisfactory bonding strength - The addition of further metallic susceptors in the bond line decreases the joint strength	[35]
Induction welding of polycarbonate, polybutyleneterephtalate, polypropylene	Emaweld® Ferromagnetic particles	- Weld strengths of 30.1 MPa (polycarbonate), 26.0 Mpa (polybutyleneterephtalate), and 17.6 MPa (polypropylene)	[36]
Induction welding of polyamide 6 containing 33 wt.% of glass fibers	Emaweld® Ferromagnetic particles	- A 25% improvement in burst strength of the joints	[37]
Induction welding of polysulfone	Ni particles	- Bond strengths comparable to those attained with a standard autoclave process but with one order of magnitude decrease in cycle times.	[38]

Table 1. *Cont.*

Application	Type of Susceptor	Main Outcomes	Ref.
Induction welding of polymethylmethacrylate	Ni-plated coating	- The best mechanical resistance of the microfluidic devices achieved by using pulse induction heating and applying 45 kPa bonding pressure	[39]
Induction welding of PEEK	Carbon fibers	- Carbon fibers act both as reinforcement and susceptor - Inhomogeneous temperature distribution because of edge effects - Appearance of different welding defects	[41]
Curing of epoxy systems	Copper or steel mesh	- Significant decrease in the curing time - Negligible effects on the mechanical behavior	[42]
Curing of epoxy systems	$FeCo/(Co,Fe)_3O_4$	- Achievement of heating rates as high as 1 K/s - Just 70 s required to reach temperatures beyond 100 °C	[43]
Curing of thiol-acrylate or thiol-ene resins	Ni nanoparticles or Co microparticles with multiwalled carbon nanotubes	- Thiol-acrylates much more reactive than thiol-ene counterparts	[44]
Curing of epoxy systems	Carbon nanotubes	- Processing conditions significantly affect the heating rates and curing times	[45]
Curing of epoxy and polyurethane systems	Curie particles	- Increase in the curing kinetics of the adhesives - Better control of the temperature during the curing processes	[46–51]
Self-healing of poly(etherurethane)	Core–shell magnetite/silica nanoparticles	- Reduced shape recovery rates	[54]
Self-healing of methacrylate-based thermosets	Fe_3O_4 nanoparticles	- Achievement of good shape memory properties, strictly related to the susceptor loading	[55]
Self-healing of poly(lactic acid)/thermoplastic polyurethane blend-healing of	Fe_3O_4 particles	- Excellent shape fix ratio (approaching 100%)—high recovery ratio (>91%) - Rapid magnetic response as short as 40 s (in the case of 30 wt.% particle loading)	[56]
Self-healing of trisfuran—pentaerythritol propoxylate tris(3-(furfurylthiol)propionate—with a bismaleimide—1,1′-(methylene-di-4,1-phenylene) bismaleimide	Chromium(IV) oxide	- Properties of the networks unchanged even after 10 cycles of damage and healing	[57]
Self-healing of anionic polyelectrolyte copolymers	Oleic acid-functionalized iron oxide particles	- Full self-repair	[58]

Table 1. *Cont.*

Application	Type of Susceptor	Main Outcomes	Ref.
Self-healing of poly(ethylene-methacrylic acid)	Fe_3O_4 nanoparticles	- Fast (<1 min) debonding and rebonding of the polymer adhesive - A 100% recovery of the original bond strength, even after five cycles of repeated debonding and rebonding	[59]
Self-healing of glass fiber-reinforced epoxy lap shear joints using ABS copolymer	Fe_3O_4 nanoparticles	- Young's modulus of ABS regained its value before damage	[60]
Self-healing of high-density polyethylene	Aluminum flakes	- A 20 vol.% of susceptors allowed a dull repairing in 20 min	[61]
Self-healing of thermoplastic polyurethane, polypropylene, polyamide 12, and polyetherketoneketone	Fe_3O_4 nanoparticles	- Self-healing achieved within 10 min for thermoplastic polyurethane, polypropylene, and polyamide 12 - Polyetherketoneketone required longer healing times and a higher nanoparticle loading (10 wt.%)	[62]
Inductively heatable mold systems	Nickel stamps equipped with nanograting structures	- The processed cyclic olefin copolymer required cycle times below 40 s	[67]
Induction heating-assisted pyrolysis of PVC	-	- Reduced dioxin production - A 85% of thermal efficiency achieved	[69]
Membrane distillation processes	Fe_3O_4 nanoparticles	- Almost doubled heating rate (2.0 °C/s) with respect to the same system without polyaniline and with the magnetite nanoparticles coated directly onto polytetrafluoroethylene membrane (1.1 °C/s)	[70]
Roller embossing processes	Ni magnetic particles	- Increased heating efficiency by 134% compared with the mold made with the unfilled polydimethylsiloxane	[71]

Legend: ABS: acrylonitrile–butadiene–styrene copolymer; PEEK: polyetheretherketone.

5. Concluding Remarks

Since the beginning of its existence, man has been searching for ever faster, more efficient, and controlled chemical and physical conversion methods. In the chemical field, this need has been fulfilled in searching for new chemical reactions, the evolution of process conditions, and the design and use of activators and catalysts.

At the same time, from a physical and engineering point of view, increasingly efficient reactors and new methods of providing the heat necessary to make reactions take place have been proposed.

More recently, partly for reasons of energy savings, environmental impact, and cost, microwave systems have been proposed. Compared with the much slower conventional methods, they also have the advantage of heating the system from the inside, provided that the employed reactors are transparent to this radiation. In addition, their use involves

a technical set-up that is not always applicable for safety reasons associated with this type of radiation.

From this point of view, induction heating seems to be an advantageous system, as evidenced by, among other things, the growth of its use in domestic settings.

Summarizing the main concepts, to use induction heating, it is necessary to have a heater consisting of a power unit and a solenoid. The current flowing inside the solenoid generates an induced magnetic field of intensity proportional to the applied current. The sample must be placed within the force lines of the magnetic field (usually within the solenoid itself). If the sample (or the reactor) is made of an electrically conducting material, the eddy current induced by the magnetic field begins to flow along the surface of the sample (or the reactor) in the opposite direction of the current flowing in the solenoid. The resulting heating is due to the Joule effect caused by the motion of charges in the material.

The eddy current, initially localized on the surface (skin effect), tends to penetrate the material's interior, causing even the deepest areas to heat up. However, too deep penetration is to be avoided, as this would result in the cancellation of the eddy currents and, thus, of the resulting heating by the Joule effect. This is one of the reasons for operating with alternating current instead of direct current. Alternating current induces a magnetic field that is itself alternating and eventually induces an eddy current that changes direction with the frequency of the applied current. It follows that, during a single cycle, the eddy current does not have time to penetrate deeply before it cancels out and begins to flow in the opposite direction. This implies that the higher the frequency of the alternating current, the shorter the persistence time of the eddy current on the surface of the material (or the reactor), and the shallower the resulting heating will be.

These phenomena happen in any electrically conducting material, whether exhibiting magnetic characteristics or not. More specifically, this is what occurs using metallic reactors (including those that can be used in flow chemistry), in which, by a process not too dissimilar from the traditional one, the reaction media are heated. However, even in these cases, the electrical induction system appears to be more efficient regarding the heating rate.

This category also includes those systems in which electrically conducting materials are embedded in reaction media that are not sensitive to the magnetic field. Among these, for example, we can mention composite materials containing carbon fibers or graphite. In this case, eddy currents are also generated on the surface of these fillers that, if they are homogeneously dispersed within the monomer or polymer matrix, induce their fast heating by contact. It is easy to foresee that the heating and temperature control of such an induction system is much more efficient than that of a system heated by conventional methods, which generally do not involve heating the material from the inside but from the surface (which may be too small compared with the volume of the medium itself).

In the case of embedded materials having magnetic properties (i.e., ferromagnetic or paramagnetic), these act as susceptors since other phenomena related to their ability to interact magnetically with the applied field are summed to the above.

In particular, these materials orient their magnetic moments with the direction of the applied field and tend to follow its changes. Given that in induction heating, the magnetic field varies in direction based on the frequency of the alternating current flowing inside the solenoid, the magnetic moments of the magnetic domains of the material will do so as well, thus generating frictional heat.

Specifically, with some exceptions, non-composite polymeric materials are not electrical conductors, and thus induction heating is usable only in particular applications mostly relegated to geometries involving thin layers of monomer or polymer in contact with an electrically conducting material, which in general could be a closed metal reactor, a tubular reactor (flow chemistry), or a flat surface (film).

Further, it is possible to envision induction heating in further applications as well. Among these, we would like to mention cure-on-demand processes and their combination with frontal polymerization (FP) [72]. Frontal polymerization is a macromolecular synthesis technique that exploits the formation of a hot polymerization front that propagates along

the reactor and can self-sustain due to the exothermicity of the polymerization reaction itself. The monomer-to-polymer conversion reaction is fast (typically from 0.5 to 5 cm/min) and proceeds from the initiation point, often consisting of a localized spot irradiated by heat or light. Induction heating would allow simultaneous initiation of polymerization at multiple areas and, thus, simultaneous formation of multiple fronts, further decreasing the processing time. In addition, one of the main problems limiting the number of monomer systems that can be polymerized via FP would be remedied. In fact, at present, polymers that melt at the temperature of the front (typically 120–180 °C) or that are soluble in the monomer with which the front is in contact are not synthesizable via FP because they generate unstable fronts, thus unable to propagate throughout the reactor. It follows that, for the most part, the systems that can be used in FP are thermosets.

We believe that induction heating could solve this issue. In fact, it would allow multiple parts of the monomer to be heated quickly, and this induced heating could be modulated in terms of time (short) and intensity (high) much more effectively than with traditional heating systems. These latter, operating in batch and in the absence of stirring, involve the formation of even high-temperature gradients and, therefore, gradients of final properties. In this view, tubular geometries would certainly be favored, and using thermoplastic materials would not represent a disadvantage since induction heating would allow them to be processed in the molten state, which would also save a great deal of energy.

That said, the major advantages of the applications of induction heating to polymeric systems remain mainly in the production and processing of composites containing conducting materials.

In particular, distinctions should be made between the composites in which the fillers are only electrically conductive and those in which the fillers act as susceptors in that they are also sensitive to the applied magnetic field.

As for materials that do not incorporate susceptors, eddy currents are generated near the reactor walls (if conductive) and around the fillers. Considering an optimal homogeneous distribution of the latter, it can be deduced how the heating occurs simultaneously throughout the material, with enormous advantages in terms of time and energy.

Finally, the case of polymeric materials containing magnetic susceptors is the one that offers the most significant possibilities for use and the greatest versatility of application as well. Generally, this involves the utilization of particles (possibly even nanometric), which combine the response to the just mentioned phenomena with the heating due to hysteresis and Néel relaxation.

Applications, for example, in the field of induced self-healing, can easily be glimpsed for this type of polymer composite material. In fact, if the material to be repaired is damaged, the presence of susceptors would allow for rapid and effective heating even internally to the material itself, such as to trigger the process of self-repair, which could take place thanks to the reaction of liquid escaping from the particles affected by the crack or the debonding and rebonding of dynamic links.

Similarly, it is possible to envision the use of the induction heating technique for the consolidation of porous materials. Namely, one possible use could be in stone materials having civil or even historical–artistic interest. Specifically, these can be hypothesized to be infiltrated with an appropriate monomer containing small susceptors. The application of induction heating would allow the polymerization of the monomer and, thus, the consolidation of the material even in depth and contactless.

Other possible applications may refer to the area of additive manufacturing, where the use of a heat source internal to the material itself could, for example, enable 3D printing in a similar way to what is now done by exploiting UV radiation, thus expanding the number of systems that can be processed.

In addition, applications are also easily foreseeable in stimulus-responsive materials, with shape memory features or temperature-responsive behavior, already mentioned in part in the text above.

Regarding the type of polymer matrix used (thermoplastic or thermoset), obtaining composite materials by IH involves the homogeneous dispersion of fillers (i.e., susceptors) and does not differ from the methods commonly used for composite production, as it exploits the same processing techniques.

Specifically, fillers incorporated into thermoplastic matrices can be processed by the standard processing techniques for thermoplastics (i.e., compounding, extrusion, and injection molding), while, in the case of thermosetting matrices, mechanical stirring and sonication will be favored.

In conclusion, the authors hope to have attracted interest from the macromolecular scientific community and hope for greater use of the induction heating technique in both established and new applications.

References

1. Saldivar-Guerra, E.; Vivaldo-Lima, E. *Handbook of Polymer Synthesis, Characterization and Processing*; John Wiley & Sons: Hoboken, NJ, USA, 2013.
2. Davies, E.J. *Conduction and Induction Heating*; Peter Peregrinus Ltd.: London, UK, 1990.
3. Bay, F.; Labbe, V.; Favennec, Y.; Chenot, J.L. A numerical model for induction heating processes coupling electromagnetism and thermomechanics. *Int. J. Numer. Meth. Eng.* **2003**, *58*, 839–867. [CrossRef]
4. Wang, W.; Tuci, G.; Duong-Viet, C.; Liu, Y.; Rossin, A.; Luconi, L.; Nhut, J.M.; Nguyen-Dinh, L.; Pham-Huu, C.; Giambastiani, G. Induction Heating: An Enabling Technology for the Heat Management in Catalytic Processes. *ACS Catal.* **2019**, *9*, 7921–7935. [CrossRef]
5. Lisjak, D.; Mertelj, A. Anisotropic Magnetic Nanoparticles: A Review of their Properties, Syntheses and Potential Applications. *Prog. Mater. Sci.* **2018**, *95*, 286–328. [CrossRef]
6. Ruffini, R.S.; Madeira, R.J. Production and Concentration of Magnetic Flux for Eddy Current Heating Applications. *Mater. Sci. Forum* **1992**, *102–104*, 383–392. [CrossRef]
7. Corcoran, J.; Nagy, P.B. Compensation of the Skin Effect in Low-Frequency Potential Drop Measurements. *J. Nondestruct. Eval.* **2016**, *35*, 58. [CrossRef]
8. Ahmed, T.J.; Stavrov, D.; Bersee, H.E.N.; Beukers, A. Induction welding of thermoplastic composites—An overview. *Compos. Part A Appl.* **2006**, *37*, 1638–1651. [CrossRef]
9. Mitschang, P.; Rudolf, R.; Neitzel, M. Continuous induction welding process, modelling and realisation. J. Thermoplast. *Comp. Mater.* **2002**, *15*, 127–153.
10. Ceylan, S.; Coutable, L.; Wegner, J.; Kirschning, A. Inductive Heating with Magnetic Materials Inside Flow Reactors. *Chem. Eur. J.* **2011**, *17*, 1884–1893. [CrossRef]
11. Wegner, J.; Ceylan, S.; Friese, C.; Kirschning, A. Inductively Heated Oxides Inside Microreactors—Facile Oxidations under Flow Conditions. *Eur. J. Org. Chem.* **2010**, *2010*, 4372–4375. [CrossRef]
12. Hartwig, J.; Ceylan, S.; Kupracz, L.; Coutable, L.; Kirschning, A. Heating under High-Frequency Inductive Conditions: Application to the Continuous Synthesis of the Neurolepticum Olanzapine (Zyprexa). *Angew. Chem. Int. Ed.* **2013**, *52*, 9813–9817. [CrossRef]
13. Fuentes, M.; Magraner, J.; De Las Pozas, C.; Roque-Malherbe, R.; Pariente, J.P.; Corma, A. Cyclization of Citronellal to Isopulegol by Zeolite Catalysis. *Appl. Catal.* **1989**, *47*, 367–374. [CrossRef]
14. Zadražil, A.; Štěpánek, F. Remote Control of Reaction Rate by Radiofrequency Heating of Composite Catalyst Pellets. *Chem. Eng. Sci.* **2015**, *134*, 721–726. [CrossRef]
15. Aasberg-Petersen, K.; Bak Hansen, J.-H.; Christensen, T.S.; Dybkjaer, I.; Seier Christensen, P.; Stub Nielsen, C.; Winter Madsen, S.E.L.; Rostrup-Nielsen, J.R. Technologies for Large-Scale Gas Conversion. *Appl. Catal. A* **2001**, *221*, 379–387. [CrossRef]

16. Meffre, A.; Mehdaoui, B.; Connord, V.; Carrey, J.; Fazzini, P.F.; Lachaize, S.; Respaud, M.; Chaudret, B. Complex Nano-objects Displaying both Magnetic and Catalytic Properties: A Proof of Concept for Magnetically Induced Heterogeneous Catalysis. *Nano Lett.* **2015**, *15*, 3241–3248. [CrossRef]

17. Bordet, A.; Lacroix, L.-M.; Fazzini, P.-F.; Carrey, J.; Soulantica, K.; Chaudret, B. Magnetically Induced Continuous CO_2 Hydrogenation Using Composite Iron Carbide Nanoparticles of Exceptionally High Heating Power. *Angew. Chem. Int. Ed.* **2016**, *55*, 15894–15898. [CrossRef] [PubMed]

18. Lucía, O.; Maussion, P.; Dede, E.J.; Burdío, J.M. Induction Heating Technology and Its Applications: Past Developments, Current Technology, and Future Challenges. *IEEE Trans. Ind. Electron.* **2014**, *61*, 2509–2520. [CrossRef]

19. Gomez-Polo, C.; Larumbe, S.; Perez-Landazabal, J.I.; Pastor, J.M. Analysis of heating effects (magnetic hyperthermia) in FeCrSiBCuNb amorphous and nanocrystalline wires. *J. Appl. Phys.* **2012**, *111*, 07A314-1–07A314-3. [CrossRef]

20. Ageorges, C.; Ye, L.; Hou, M. Advances in fusion bonding techniques for joining thermoplastic matrix composites: A review. *Compos. Part A Appl.* **2001**, *32*, 839–857. [CrossRef]

21. Yousefpour, A.; Hojjati, M.; Immarigeon, J.P. Fusion bonding/welding of thermoplastic composites. *J. Therm. Compos. Mater.* **2004**, *17*, 303–341. [CrossRef]

22. Stokes, V.K. Joining methods for plastics and plastic composites: An overview. *Polym. Eng. Sci.* **1989**, *29*, 1310–1324. [CrossRef]

23. Rotheiser, J. *Joining of Plastics*; Hanser: München, Germany, 2009; pp. 335–350.

24. Grewell, D.; Benatha, A.; Park, J.B. *Plastics and Composites Welding Handbook*; Hanser: München, Germany, 2003; pp. 109–121.

25. Troughton, M.J. *Handbook of Plastics Joining: A Practical Guide*; William Andrew Inc.: Norwich, UK, 2008; pp. 113–120.

26. Lambiase, F.; Balle, F.; Blaga, L.A.; Liu, F.; Amancio-Filho, S.T. Friction-based processes for hybrid multi-material joining. *Compos. Struct.* **2021**, *266*, 113828. [CrossRef]

27. Iftikhar, S.H.; Mourad, A.H.I.; Sheikh-Ahmad, J.; Almaskari, F.; Vincent, S. A Comprehensive Review on Optimal Welding Conditions for Friction Stir Welding of Thermoplastic Polymers and Their Composites. *Polymers* **2021**, *13*, 1208. [CrossRef] [PubMed]

28. Velmurugan, P.; Manohar, J.; Kannan, C.R.; Manivannan, S.; Vairamuthu, J.; Stalin, P.; Stalin, B. A Study on Development of Induction Welding of Thermoplastic Composites. *IOP Conf. Ser. Mater. Sci. Eng.* **2020**, *988*, 012109. [CrossRef]

29. Mitschang, P.; Velthuis, R.; Didi, M. Induction spot welding of metal CFRPC hybrid joints. *Adv. Eng. Mater.* **2013**, *15*, 804–813. [CrossRef]

30. Mitschang, P.; Velthuis, R.; Emrich, S.; Kopnarski, M. Induction heated joining of aluminum and carbon fibre reinforced nylon 66. *J. Therm. Compos. Mater.* **2009**, *22*, 767–801. [CrossRef]

31. Rudolf, R.; Mitschang, P.; Neitzel, M. Induction heating of continuous carbon fibre-reinforced thermoplastics. *Compos. Part A Appl.* **2000**, *31*, 1191–1202. [CrossRef]

32. Moser, L. *Experimental Analysis and Modelling of Susceptorless Induction Welding of High Performance Thermoplastic Polymer Composites*; IVW GmbH: Kaisersalutern, Germany, 2012.

33. Keller, R.; Schmidbauer, E. Magnetic properties and rotational hysteresis losses of oxidized 250 nm Fe_3O_4 particles. *J. Magn. Magn. Mater.* **1996**, *162*, 85–90. [CrossRef]

34. Becker, S.; Mitschang, P. Process Improvement of Continuous Induction Welding of Carbon Fiber-Reinforced Polymer Composites. *J. Mater. Eng. Perform.* **2022**, *31*, 7049–7060. [CrossRef]

35. Border, J.; Salas, R. Induction heated joining of thermoplastic composites without metal susceptors. In Proceedings of the 34th International SAMPE Symposium, Reno, NV, USA, 8–11 May 1989; pp. 2569–2578.

36. Stokes, V.K. Experiments on the induction welding of thermoplastics. *Polym. Eng. Sci.* **2003**, *43*, 1523–1541. [CrossRef]

37. Kagan, V.A.; Nichols, R.J. Benefits of induction welding of reinforced thermoplastics in high performance applications. *J. Reinf. Plast. Compos.* **2005**, *24*, 1345–1352. [CrossRef]

38. Suwanwatana, W.; Yarlagadda, S.; Gillespie Jr, J.W. Hysteresis heating based induction bonding of thermoplastic composites. *Compos. Sci. Technol.* **2006**, *66*, 1713–1723. [CrossRef]

39. Knauf, B.J.; Webb, D.P.; Liu, C.C.; Conway, P.P. Low frequency induction heating for the sealing of plastic microfluidic systems. *Microfluid. Nanofluid* **2010**, *9*, 243–252. [CrossRef]

40. Martin, R.G.; Johansson, C.; Tavares, J.R.; Dubé, M. Material Selection Methodology for an Induction Welding Magnetic Susceptor Based on Hysteresis Losses. *Adv. Eng. Mater.* **2022**, *24*, 2100877. [CrossRef]

41. Wang, F.; Zhang, P.; Luo, J.; Li, B.; Liu, G.; Zhan, X. Effect of heat input on temperature characteristics and fusion behavior at bonding interface of CFRTP induction welded joint with carbon fiber susceptor. *Polym. Compos.* **2023**, *44*, 1586–1602. [CrossRef]

42. Fink, B.K.; McKnight, S.H.; Yarlagadda, S.; Gillespie, J.W., Jr. *Non-Polluting Composites Repair and Remanufacturing for Military Applications: Induction-Based Repair of Integral Armor, ARL-TR-2121*; Army Research Laboratory: Aberdeen, MD, USA, 1999.

43. Miller, K.J.; Collier, K.N.; Soll-Morris, H.B.; Swaminathan, R.; McHenry, M.E. Induction heating of FeCo nanoparticles for rapid rf curing of epoxy composites. *J. Appl. Phys.* **2009**, *105*, 07E714. [CrossRef]

44. Ye, S.; Cramer, N.B.; Stevens, B.E.; Sani, R.L.; Bowman, C.N. Induction curing of thiol-acrylate and thiol-ene composite systems. *Macromolecules* **2011**, *44*, 4988–4996. [CrossRef]

45. Vashisth, A.; Healey, R.E.; Pospisil, M.J.; Oh, J.H.; Green, M.J. Continuous processing of pre-pregs using radio frequency heating. *Compos. Sci. Technol.* **2020**, *195*, 108211. [CrossRef]

46. Voß, M.; Vallée, T. Accelerated curing of G-FRP rods glued into timber by means of inductive heating—Influences of curing kinetics. *J. Adhes.* **2022**, *98*, 1037–1075. [CrossRef]

47. Voß, M.; Vallée, T.; Kaufmann, M. Accelerated curing of adhesively bonded G-FRP tube connections—Part III: Modelling of strength. *Compos. Struct.* **2021**, *268*, 113900. [CrossRef]

48. Voß, M.; Haupt, J. Accelerated curing of adhesively bonded g-frp tube connections part I: Experimental investigation. *Compos. Struct.* **2021**, *268*, 113999. [CrossRef]

49. Voß, M.; Evers, T.; Vallée, T. Low-temperature curing of adhesives—Large-scale experiments. *J. Adhes.* **2023**, *99*, 817–852. [CrossRef]

50. Voß, M.; Kaufmann, M.; Vallée, T. Curie-supported accelerated curing by means of inductive heating—Part I: Model building. *J. Adhes.* **2022**, *98*, 1394–1437. [CrossRef]

51. Voß, M.; Kaufmann, M.; Vallée, T. Curie–supported accelerated curing by means of inductive heating—Part II Validation and numerical studies. *J. Adhes.* **2022**, *98*, 2045–2077. [CrossRef]

52. Xia, Y.; He, Y.; Zhang, F.; Liu, Y.; Leng, J. A Review of Shape Memory Polymers and Composites: Mechanisms, Materials, and Applications. *Adv. Mater.* **2021**, *33*, 2000713. [CrossRef]

53. Wang, S.; Urban, M.W. Self-healing polymers. *Nat. Rev. Mater.* **2020**, *5*, 562–583. [CrossRef]

54. Mohr, R.; Kratz, K.; Weigel, T.; Lucka-Gabor, M.; Moneke, M.; Lendlein, A. Initiation of shape-memory effect by inductive heating of magnetic nanoparticles in thermoplastic polymers. *Proc. Natl. Acad. Sci. USA* **2006**, *103*, 3540–3545. [CrossRef]

55. Yakacki, C.; Satarkar, N.S.; Gall, K.; Likos, R.; Hilt, J.Z. Shape-memory polymer networks with Fe_3O_4 nanoparticles for remote activation. *J. Appl. Polym. Sci.* **2009**, *112*, 3166–3176. [CrossRef]

56. Liu, H.; Wang, F.; Wu, W.; Dong, X.; Sang, L. 4D printing of mechanically robust $PLA/TPU/Fe_3O_4$ magneto-responsive shape memory polymers for smart structures. *Compos. B Eng.* **2023**, *248*, 110382. [CrossRef]

57. Adzima, B.J.; Kloxin, C.J.; Bowman, C.N. Externally triggered healing of a thermoreversible covalent network via self-limited hysteresis heating. *Adv. Mater.* **2010**, *22*, 2784–2787. [CrossRef]

58. Oberhausen, B.; Kickelbick, G. Induction heating induced self-healing of nanocomposites based on surface-functionalized cationic iron oxide particles and polyelectrolytes. *Nanoscale Adv.* **2021**, *3*, 5589–5604. [CrossRef]

59. Cheng, X.; Zhou, Y.; Charles, A.D.M.; Yu, Y.; Islam, M.S.; Peng, S. Enabling contactless rapid on-demand debonding and rebonding using hysteresis heating of ferrimagnetic nanoparticles. *Mater. Des.* **2021**, *210*, 110076. [CrossRef]

60. Palanisamy, R.P.; Karpenko, O.; Vattathurvalappil, S.H.; Deng, Y.; Udpa, L.; Haq, M. Guided wave monitoring of Nano-Fe_3O_4 reinforced thermoplastic adhesive in manufacturing of reversible composite lap-joints using targeted electromagnetic heating. *NDT&E Int.* **2021**, *122*, 102481.

61. Waldman, L.J.; Keller, M.W. Remendable conductive polyethylene composite with simultaneous restoration of electrical and mechanical behavior. *Polym. Eng. Sci.* **2022**, *62*, 991–998. [CrossRef]

62. Kanidi, M.; Loura, N.; Frengkou, A.; Kosanovic Milickovic, T.; Trompeta, A.F.; Charitidis, C. Inductive Thermal Effect on Thermoplastic Nanocomposites with Magnetic Nanoparticles for Induced-Healing, Bonding and Debonding On-Demand Applications. *J. Compos. Sci.* **2023**, *7*, 74. [CrossRef]

63. Feigenblum, J.; Senmartin, J. RTM technology improvement with tool surface heating by induction. In Proceedings of the 9th International Conference on Flow Processes in Composites Materials (FPCM-9), Montréal, QC, Canada, 8–10 July 2008.

64. Bayerl, T.; Duhovic, M.; Mitschang, P.; Bhattacharyya, D. The heating of polymer composites by electromagnetic induction—A review. *Compos. Part A Appl.* **2014**, *57*, 27–40. [CrossRef]

65. Guichard, A.; Feigenblum, J. Induction heating for high speed RTM process. *JEC Compos. Mag.* **2007**, *31*, 40–43.

66. Chen, S.C.; Jong, W.R.; Chang, J.A. Dynamic mould surface temperature control using induction heating and its effect on the surface appearance of weld line. *J. Appl. Polym. Sci.* **2006**, *101*, 1174–1180. [CrossRef]

67. Kim, S.; Shia, C.S.; Kim, B.H.; Yao, D. Injection moulding nanoscale features with the aid of induction heating. *Polym. Plast. Technol. Eng.* **2007**, *46*, 1031–1037. [CrossRef]

68. Tanaka, K.; Katsura, T.; Kinoshita, Y.; Katayama, T. Mechanical properties of jute fabric reinforced thermoplastic moulded by high-speed processing using electromagnetic induction. *High Perform. WIT Trans. Built Environ.* **2008**, *97*, 211–219.

69. Nakanoh, K.; Hayashi, S.; Kida, K. Waste Treatment Using Induction-Heated Pyrolysis. *Fuji Electr. Rev.* **2008**, *47*, 69–73.

70. Qing, W.; Hu, Z.; Ma, Q.; Zhang, W. Conductive Fe_3O_4/PANI@PTFE membrane for high thermal efficiency in interfacial induction heating membrane distillation. *Nano Energy* **2021**, *89*, 106339. [CrossRef]

71. Hsu, M.H.; Tsai, Y.Y.; He, J.W.; Yang, S.Y. Induction heating of dual magnetic particles embedded PDMS molds for roller embossing applications. *Microsyst. Technol.* **2023**, *29*, 405–415. [CrossRef]

72. Suslick, B.A.; Hemmer, J.; Groce, B.R.; Stawiasz, K.J.; Geubelle, P.H.; Malucelli, G.; Mariani, A.; Moore, J.S.; Pojman, J.A.; Sottos, N.R. Frontal Polymerizations: From Chemical Perspectives to Macroscopic Properties and Applications. *Chem. Rev.* **2023**, *123*, 3237–3298. [CrossRef] [PubMed]